DOI: 10.1002/ejic.201100589

Homopiperazine and Piperazine Complexes of Zr^{IV} and Hf^{IV} and Their Application to the Ring-Opening Polymerisation of Lactide

Stuart L. Hancock,[a] Mary F. Mahon,[a] Gabriele Kociok-Kőhn,[a] and Matthew D. Jones*[a]

Keywords: Titanium / Zirconium / Hafnium / Ring-opening polymerization / Sustainable chemistry

In this paper we describe the preparation and characterisation, by single-crystal X-ray diffraction, of twelve Zr^{IV}/Hf^{IV} complexes based on piperazine or homopiperazine salan ligands. With the piperazine ligands, a mixture of species was observed and various solid-state structures were isolated. However, with homopiperazine salan ligands, 1:1 ligand-to-metal complexes were observed both in solution and in the solid state. Interestingly, for the homopiperazine complexes the isopropoxide ligands are *trans* to one another in the solid state, most likely because of the rigid nature of the homopiperazine backbone. All homopiperazine Hf^{IV} and Zr^{IV} complexes were tested for the ring-opening polymerisation (ROP) of *rac*-lactide. The complexes are active and produce polylactide with narrow polydispersity indices. The kinetics and living characteristics of the polymerisation have also been investigated.

Introduction

In recent years there has been an explosion of interest in the use of single-site homogeneous catalysts for the ring-opening polymerisation (ROP) of *rac*-lactide (*rac*-LA) to produce polylactide (PLA).[1] This process has been commercialised by Purac and NatureWorks, and the current catalyst used for this process is based on Sn^{II}.[2] There is currently a desire to replace tin in this system, and – as a consequence – a significant amount of work has been performed in catalyst development.[1] The polymers themselves have found extensive utility from biomedical to commodity polymer applications,[3] due to the biodegradability and biocompatibility of PLA and the fact that the monomer can be sourced from sustainable raw materials. The catalyst can have a dramatic effect on the physical properties and degradation rates of the resultant PLA.[4] For example, catalysts based on groups 1–3,[5] lanthanides,[6] Zn^{II},[1a,1b,1g] Al^{III},[7] In^{III}[8] and, pertinent to this study, group 4 metals have all been shown to have significant activity.[9] We have recently shown that Ti^{IV} salan systems with a piperazine backbone are very effective catalysts for the bulk polymerisation of *rac*-LA.[10] Kol has shown that a Zr^{IV} complex of a tetradentate phenylenediamine bis(phenolate) affords heterotactic PLA under melt conditions.[11] The same group has also shown that dithiodiolate complexes with Zr^{IV} are active for the production of hetereotactic PLA.[9h] It has been shown that dinuclear Zr^{IV} and Hf^{IV} complexes of Jacobsen's ligand are active for the controlled ROP of both *rac*-LA and β-butyrolactone.[9a] In the case of *rac*-LA, atactic PLA was formed. It has also been shown that bis(imino)phenoxide complexes of Zr^{IV} show high activities in the polymerisation.[9g]

The chemistry of group 4 metal complexes with symmetrical amine–bis(phenolate) ligands is rich and diverse, and many ligand–metal complexes are known with possible geometries shown in Scheme 1.[12] The use of bis(phenolate) ligands based on 2,2′-bipyrrolidine, *N*,*N*′-dimethyl-1,2-diaminobenzene, *N*,*N*′-dimethyl-1,2-ethylenediamine and *N*,*N*′-dimethylcyclohexane-1,2-diamine backbones forms the α-cis isomer both in the solid state and solution once reacted with $Zr(OtBu)_4$.[13] Interestingly, a search of the Cambridge Structural Database (CSD) indicates that there are no crystallographically characterised complexes of the *trans* isomer of group 4 metal complexes with amine bis(phenolate) ligands, where X = alkoxide, with the α-*cis* and β-*cis* forms being prevalent.[14] Intriguingly, Budzelaar has shown, using computational methods, that the *trans* geometry (*mer*–*mer*, where the ligand occupies the equatorial position) is the intermediate ion pair in olefin polymerisation.[15] The use of homopiperazine as a backbone for bis(phenolate) ligands remains limited with the only examples characterised in the solid state involving copper, nickel and iron.[16]

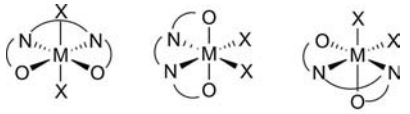

Scheme 1. Possible isomers of ONNO ligands with Zr^{IV} or Hf^{IV}.

[a] Department of Chemistry, University of Bath,
Claverton Down, Bath BA2 7AY, United Kingdom
Fax: +44-01225-386231
E-mail: mj205@bath.ac.uk

Supporting information for this article is available on the WWW under http://dx.doi.org/10.1002/ejic.201100589.

Results and Discussion

Synthesis and Characterisation of Ligands and Complexes

Our initial attempts focused on salan ligands ($\mathbf{1}H_2$–$\mathbf{3}H_2$) based on a piperazine backbone (Scheme 2). The ligands are readily prepared by a modified Mannich reaction.[10] One equivalent of the ligand was treated with one equivalent of either $Zr(OiPr)_4OHiPr$ or $Hf(OiPr)_4OHiPr$. We have previously shown that dimers can be formed in the solid state with such ligands and Ti^{IV} centres.[10]

Using the piperazine ligand, three different structural motifs were isolated in the solid state. From the reaction of $\mathbf{1}H_2$ with Zr^{IV} a tetramer was observed (Figure 1). There are two crystallographically unique Zr^{IV} centres, which are both in pseudo-octahedral environments. The phenoxide oxygen atom O1 bridges between Zr1 and Zr2 with N1 binding to Zr1. Zr2 has three terminal isopropoxide ligands with Zr–O distances ranging from 1.944(3) to 1.953(3) Å. A coordinated 2-propanol with O6 completes the coordination sphere of Zr2 with a Zr2–O6 distance of 2.287(3) Å. There is an H-bonding interaction between the alcoholic proton attached to O6 and an oxygen acceptor of a neighbouring isopropoxide unit.

Attempts then turned to $\mathbf{2}H_2$, which again has a methyl group *ortho* to the phenoxide. In this case Zr^{IV} crystals of a dimeric complex were isolated, where there are two crystallographically unique Zr^{IV} centres; Zr1 is six-coordinate and Zr2 seven-coordinate, Figure 1. Zr1 has three terminal isopropoxide groups, two bridging isopropoxide groups and one bridging phenoxide moiety, with a Zr1–O4 distance of 2.286(4) Å. Zr2 is bound to two bridging isopropoxides, two amine nitrogen atoms with distances Zr2–N1 2.481(5) and Zr2–N2 2.450(6) Å, and N1–Zr2–N2 is 59.44(18)°; a terminal isopropoxide and phenoxide complete the coordination sphere of Zr2. Zr^{IV} dimers with bis(phenoxide) salan ligands are rare and this is the first example of a tetrameric species.[9d,17] Examples with similar ligands include those of Gibson who has observed dimers with ONN ligands,[17] we have observed dimers with tris(phenolate) ligands[18] and Sun has observed dinuclear species with ONNO ligands.[9d] Upon reacting $Hf(OiPr)_4(OHiPr)$ with $\mathbf{1}H_2$ and $\mathbf{3}H_2$ a further dimeric species was observed in the solid state (Figure 2).

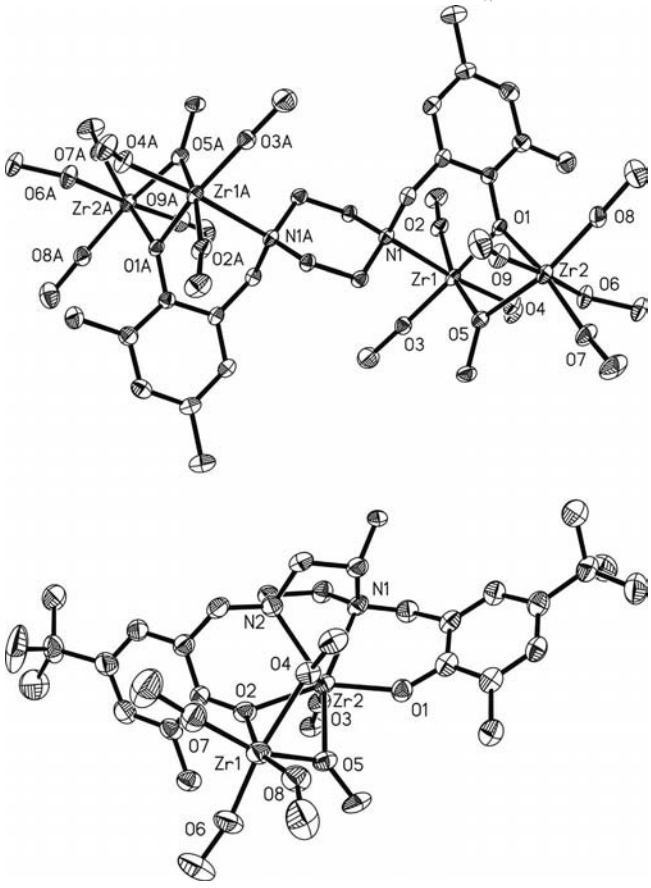

Figure 1. Solid-state structures of $Zr_4(\mathbf{1})(OiPr)_{14}(HOiPr)_2$ (top) and $Zr_2(\mathbf{2})(OiPr)_6$ (bottom). The methyl groups of the *i*Pr moieties and all hydrogen atoms have been removed for clarity. The ellipsoids are shown at the 30% probability level.

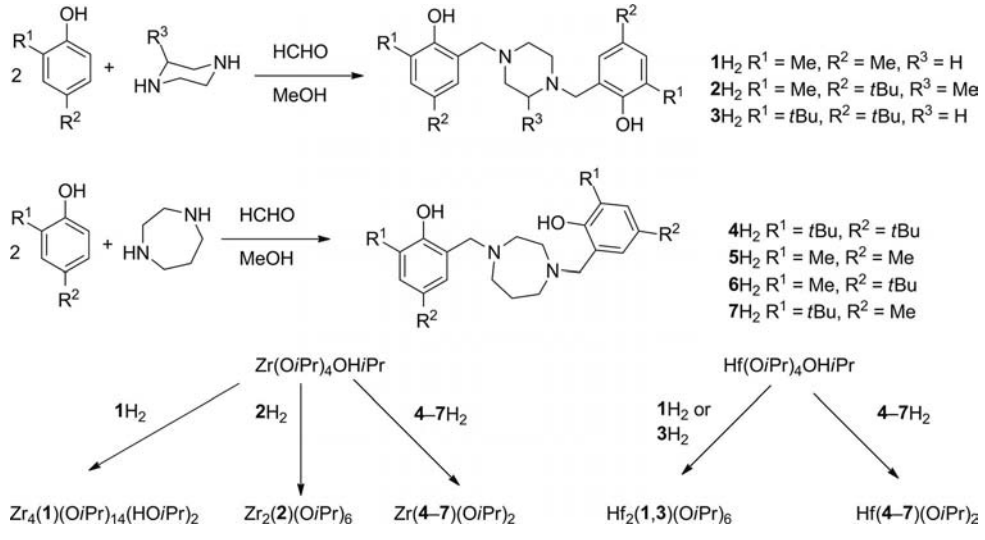

Scheme 2. Ligands and complexes prepared in this study.

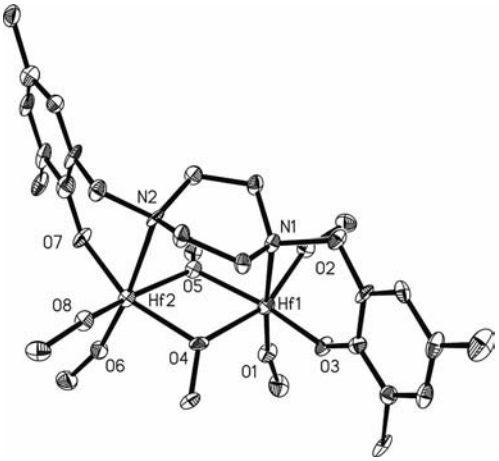

Figure 2. Solid-state structure of Hf_2(**1**)($OiPr)_6$. The methyl groups of the *i*Pr moieties and all hydrogen atoms have been removed for clarity. The ellipsoids are shown at the 30% probability level.

The motif in this case is based on each Hf^{IV} centre being bound to two terminal isopropoxide species, a terminal phenoxide, a nitrogen atom of the piperazine ring and two bridging isopropoxide moieties. This structure is analogous to that recently reported by Kol for Ti^{IV} and Zr^{IV} phenylenediamine bis(phenolate) species.[11] However, this is the first example of such a structure with Hf^{IV}. Selected bond lengths and angles for the Hf^{IV} complexes are shown in Table 1.

Table 1. Selected bond lengths (Å) and angles (°) for Hf_2(**1**)($OiPr)_6$ and Hf_2(**3**)($OiPr)_6$.

	Hf_2(**1**)($OiPr)_6$	Hf_2(**3**)($OiPr)_6$
Hf1–O1	1.908(9)	1.917(7)
Hf1–O2	1.913(10)	1.929(9)
Hf1–O3	1.995(9)	2.009(6)
Hf1–O4	2.204(10)	2.152(10)
Hf1–O5	2.122(9)	2.180(11)
Hf1–N1	2.548(12)	2.534(9)
N1–Hf1–O1	173.9(4)	169.6(3)
O5–Hf1–O4	71.2(3)	71.8(3)

For the Zr^{IV} piperazine species, the crystallised yields of these complexes were poor (ca. 5%) and NMR spectroscopic analysis of the crude reaction mixture before recrystallisation implied that a plethora of species were present as well as unreacted starting materials. The rigidity of the ligands and size of Zr^{IV} implies that various combinations and ratios of metal-to-ligand can be observed for these piperazine complexes. This is in direct contrast to our previously reported Ti^{IV} systems.[10] For the Hf^{IV} piperazine systems, the complexes were highly soluble in hexane and common organic solvents, therefore, obtaining pure material by recrystallisation proved troublesome. However, from the solution ^{1}H NMR spectra it would appear that the 1:2 solid-state forms are also the main product in solution. Attempts to increase the yields/purities for both the Zr^{IV} and Hf^{IV} systems (varying temperature, order and speed of addition of the salan ligand) were unsuccessful in increasing the purity of the final product. Therefore, attempts turned to ligands **4**H_2–**7**H_2 (Scheme 2) with the aim of producing complexes in higher purities for further polymerisation studies. The homopiperazine ligands were treated with 1 equiv. of either $Zr(OiPr)_4OHiPr$ or $Hf(OiPr)_4OHiPr$ in CH_2Cl_2, and good yields of pure 1:1 monomeric materials were obtained after recrystallisation, see Figure 3 and Table 2 for selected bond lengths and angles. We hypothesise that formation of monomers for **4**H_2–**7**H_2 is a consequence of the reduced rigidity in the homopiperazine ring compared to the piperazine ring.

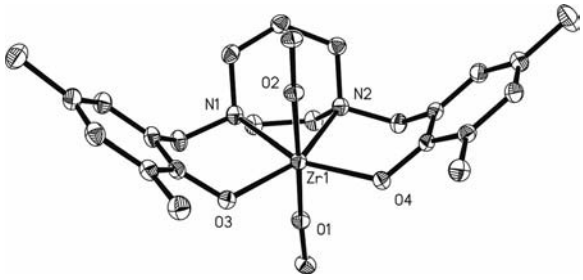

Figure 3. Solid-state structure of Zr(**5**)($OiPr)_2$. The methyl groups of the *i*Pr moieties and all hydrogen atoms have been removed for clarity. The ellipsoids are shown at the 30% probability level.

Table 2. Selected bond lengths (Å) and angles (°) for the homopiperazine solid-state structures described in this work.

	Hf(**4**)($OiPr)_2$	Zr(**5**)($OiPr)_2$	Zr(**5**)($OiPr)_2$·1/2(C_4H_8O)·1/2(C_3H_8O)
M1–O1	1.982(3)	1.9689(14)	1.9708(17)
M1–O2	1.966(3)	1.9665(14)	1.9652(16)
M1–O3	2.037(3)	2.0476(15)	2.0950(17)
M1–O4	2.037(3)	2.0567(14)	2.1292(15)
M1–O5	–	–	2.469(10)
M1–N1	2.340(4)	2.3958(18)	2.4831(19)
M1–N2	2.349(3)	2.3876(18)	2.4945(18)
O1–M1–O2	176.36(13)	174.71(6)	169.18(7)
O3–M1–O4	119.36(12)	121.40(6)	137.96(6)
N1–M1–N2	67.27(12)	66.40(6)	63.79(6)
Ph–Ph planes	108.2	104.4	104.7
	Hf(**5**)($OiPr)_2$	Zr(**6**)($OiPr)_2$	Hf(**6**)($OiPr)_2$
M1–O1	1.960(4)	1.968(4)	1.957(7)
M1–O2	1.955(4)	1.964(4)	1.993(6)
M1–O3	2.030(4)	2.041(2)	2.040(2)
M1–O4	2.041(4)	–	–
M1–O5	–	–	–
M1–N1	2.357(5)	2.387(3)	2.363(3)
M1–N2	2.364(5)	–	–
O1–M1–O2	174.83(16)	173.5(2)	172.7(4)
O3–M1–O4	119.17(15)	119.57(13)[a]	117.34(13)[a]
N1–M1–N2	66.65(16)	66.70(13)	67.46(13)
Ph–Ph planes	105.1	98.8	98.9

[a] Due to symmetry, this angle is O3–M1–O3A.

The ligands chosen impart varying steric constraints around the metal centre. In these cases monomeric species are formed in the solid state with the ONNO atoms of the ligands occupying the equatorial plane and the isopropoxide groups are *trans* to one another with an *i*PrO–M–O*i*Pr angle of approximately 175°. As a consequence the phenoxide groups are *cis* to each other as are the amine groups. This is in stark contrast to all amine bis(phenolate) (and

OSSO) Zr^{IV} or Hf^{IV} isopropoxide complexes in the CSD.[14,19] However, such species have been observed for Ti^{IV} in solution.[12] Noteworthy, in dichloro species it is more common for the ligand to occupy the equatorial sites and the chloro in the axial positions.[20] The formation of these *trans* complexes must be related to the fact that the ligands are not as flexible as the majority of salen or salan complexes used to date. The ligand is considerably distorted from planarity with the phenyl rings forming a bowl-like arrangement around the metal centre with isopropoxide O2 encapsulated in the bowl (Figure 3). This can be quantified by the angle between the planes formed by the two phenoxide rings of ca. 100° (Table 2). The O3–M–O4 angles are approximately 120°, indicating that there is a significant opportunity for further coordination. Moreover, when the crude product from the reaction of **5**H_2 with Zr^{IV} is recrystallised from THF and hexane, this vacant site becomes occupied (Figure 4). The Zr^{IV} centre is now coordinated to a molecule of either THF or 2-propanol, and it is consequently seven-coordinate; these solvents are both half-occupied in the solid-state structure. Due to this extra ligand and increased coordination number the Zr^{IV}–O/N distances of the salan ligands become significantly elongated compared to those of the six-coordinate complexes. As expected O3–M–O4 is more obtuse at 137.96(6)°, as the ligand adjusts itself to accommodate the coordination of the solvent. This bodes well for ROP as it is generally assumed that the first step is the coordination of the monomer to the metal centre.[3a]

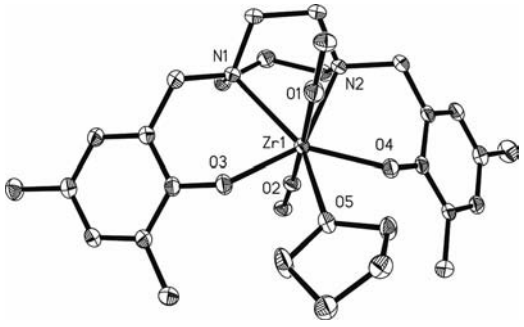

Figure 4. Solid-state structure of Zr(**5**)(O*i*Pr)$_2$·1/2THF·1/2IPA. The methyl groups of the *i*Pr moieties, the half-occupied 2-propanol and all hydrogen atoms have been removed for clarity. The ellipsoids are shown at the 30% probability level.

The room temperature ^{1}H NMR spectra of these 1:1 species are complex and broad resonances are observed for the methylene CH_2 moieties. Upon cooling, the spectra sharpen and clearly defined resonances are seen for the methylene groups, two isopropoxide groups are observed, one of which is significantly upfield from typical Zr/Hf-O*i*Pr resonances, with a methyl resonance close to 0 ppm. This is presumably the isopropoxide group in the bowl, which is in close proximity (ca. 2.8 Å from the phenyl ring centroid to the CH_3 hydrogen atoms) to the two electron rich phenyl rings causing these to be more shielded. Analysis of both the ^{1}H and ^{13}C{^{1}H} NMR spectra indicate that the solid-state structures are maintained in solution.

Polymerisation of *rac*-LA

The monomeric complexes were tested for the ROP of *rac*-LA under solvent-free (Table 3) and solution (Table 4) conditions. In the melt, high molecular weight PLA is obtained and in some cases there is a slight isotactic bias to the resultant polymer, the highest being P_m = 0.63 for Hf(**5**)(O*i*Pr)$_2$. If the theoretical molecular weight is compared to the measured M_n for Zr^{IV}/Hf^{IV} catalysts, for entries 1, 2, 4, 5, 6 and 7 two polymer chains grow per metal centre whereas for entries 3, 8, 9, 10 one chain grows per metal centre. To achieve high conversion with complexes based on **4**H_2 and **7**H_2 (*ortho*-*t*Bu group) then longer times, 3 h, were required compared to ligands with *ortho*-Me groups, which only required 30 min to achieve high conversions. A plot of M_n/PDI vs. conversion for Hf(**4**)(O*i*Pr)$_2$ shows a linear increase in molecular weight with conversion and the PDI remains relatively constant (Figure 5). When the monomer-to-initiator ratio was increased to 900:1 (entries 2 and 7, Table 3) then the molecular weight increased in a predictable fashion. However, the conversions were significantly lower, which could be caused by the increased viscosity as the molecular weight increases.

Table 3. Melt polymerisation data for Zr/Hf(**4**–**7**)(O*i*Pr)$_2$ at a monomer/initiator ratio of 300:1 (1 g of monomer was used in all cases at 130 °C).

Entry		Time (h)	Conversion[a]	M_n[b]	PDI[b]	P_m[c]
1	Zr(**4**)(O*i*Pr)$_2$	3	86	20900	1.22	0.49
2	Zr(**4**)(O*i*Pr)$_2$	6[d]	48	31950	1.12	0.44
3	Zr(**5**)(O*i*Pr)$_2$	0.5	97	45000	1.39	0.56
4	Zr(**6**)(O*i*Pr)$_2$	0.5	79	15200	1.17	0.49
5	Zr(**7**)(O*i*Pr)$_2$	3	89	19325	1.31	0.53
6	Hf(**4**)(O*i*Pr)$_2$	3	87	26000	1.14	0.50
7	Hf(**4**)(O*i*Pr)$_2$	6[d]	41	28825	1.15	0.44
8	Hf(**5**)(O*i*Pr)$_2$	0.5	91	47825	1.33	0.63
9	Hf(**6**)(O*i*Pr)$_2$	0.5	96	37150	1.28	0.61
10	Hf(**7**)(O*i*Pr)$_2$	3	90	35600	1.32	0.50

[a] Conversion determined by ^{1}H NMR spectroscopy. [b] Determined from GPC analysis with THF as the solvent. [c] Determined from ^{1}H NMR homonuclear decoupled NMR spectroscopy. [d] Monomer/initiator ratio 900:1.

Table 4. Solution polymerisation data for Zr/Hf(**4**–**7**)(O*i*Pr)$_2$ at a monomer/initiator ratio of 100:1 (1 g of monomer was dissolved in 10 mL of toluene in all cases at 80 °C).

Entry		Time (h)	Conversion[a]	M_n[b]	PDI[b]	P_m[c]
1	Zr(**4**)(O*i*Pr)$_2$	24	79	7975	1.21	0.55
2	Zr(**5**)(O*i*Pr)$_2$	24	96	10025	1.69	0.62
3	Zr(**5**)(O*i*Pr)$_2$	24[d]	97	45700	1.59	0.62
4	Zr(**6**)(O*i*Pr)$_2$	24	93	10550	1.55	0.58
5	Zr(**7**)(O*i*Pr)$_2$	24	26	4400	1.22	–
6	Hf(**4**)(O*i*Pr)$_2$	24	12	1650	1.05	–
7	Hf(**5**)(O*i*Pr)$_2$	24	95	12825	1.68	0.63
8	Hf(**5**)(O*i*Pr)$_2$	24[d]	94	52100	1.20	0.65
9	Hf(**6**)(O*i*Pr)$_2$	6	83	9275	1.11	0.63
10	Hf(**7**)(O*i*Pr)$_2$	24	22	2550	1.26	0.48

[a] Conversion determined by ^{1}H NMR spectroscopy. [b] Determined from GPC analysis using THF as the solvent. [c] Determined from ^{1}H NMR homonuclear decoupled NMR spectroscopy. [d] Monomer/initiator ratio 300:1.

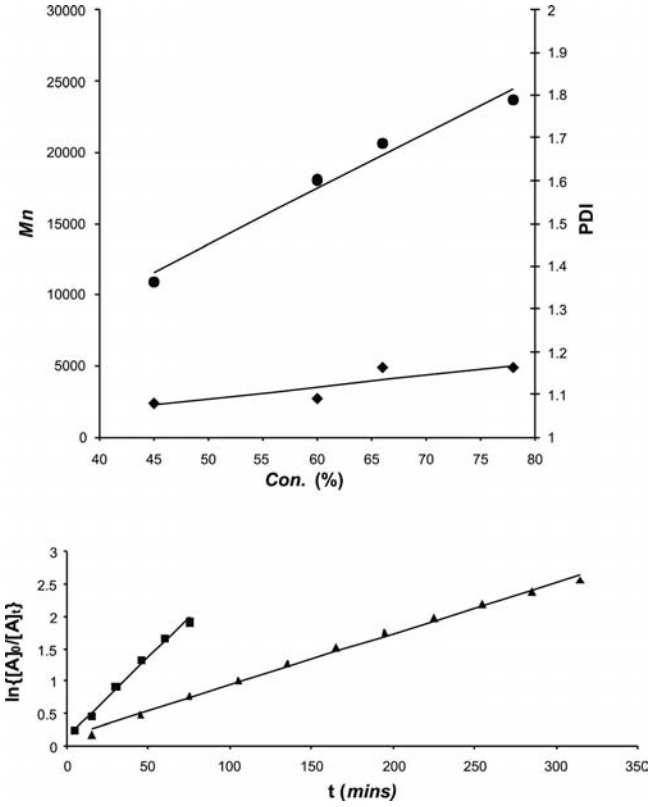

Figure 5. M_n/PDI vs. time for melt polymerisation with Hf(**4**)-(O*i*Pr)$_2$ (circles = M_n, diamonds = PDI) (top). Solution kinetics for Zr(**5**)(O*i*Pr)$_2$ (squares, k_{app} = 0.025 min^{-1}, R^2 = 0.9928) and Hf(**5**)(O*i*Pr)$_2$ (triangles, k_{app} = 0.008 min^{-1}, R^2 = 0.9956) (bottom).

The solution polymerisation of these Zr^{IV} and Hf^{IV} homopiperazine complexes are more controlled than with Ti^{IV} homopiperazine complexes.[10] In certain cases under solution conditions, a slight isotactic bias was observed for the PLA (Table 4). Interestingly, the tacticity observed in this study with these *trans* complexes is lower than that seen previously with α-*cis* group 4 salan complexes.[1c] Analysis of the molecular weight data implies that one chain grows per metal centre. As observed with the melt conditions, the presence on an *ortho*-*t*Bu group appears to slow the polymerisation in solution dramatically with significantly lower conversions after 24 h for complexes prepared from **4**H$_2$ and **7**H$_2$ (entries 1, 5, 6 and 10, Table 4) presumably due to steric arguments. When the monomer-to-initiator ratio was increased (entries 3 and 8, Table 4) the molecular weight increased accordingly. MALDI-ToF mass spectrometry indicated the presence of H and O*i*Pr end groups for the solution polymerisations, as expected with the coordination insertion mechanism. Pseudo first order solution kinetics were investigated for Zr(**5**)(O*i*Pr)$_2$ (k_{app} = 0.025 min^{-1}) and Hf(**5**)(O*i*Pr)$_2$ (k_{app} = 0.008 min^{-1}), and the Zr^{IV} complex is three times faster than the Hf^{IV} complex. This is in agreement with previous work, which indicates that Zr^{IV} initiators tend to be faster acting than the analogous Hf^{IV} complexes.[9c,9g] Also noteworthy is the fact that the polymerisation does not show any significant induction period.

Conclusions

A series of Zr^{IV} and Hf^{IV} complexes based on piperazine and homopiperazine ligands have been prepared and characterised in the solid state to reveal that the isopropoxide groups are in *trans* positions. From NMR spectroscopic analysis, this structure is maintained in solution. The complexes have been shown to catalyse the ROP of *rac*-LA to afford PLA in a predictable fashion with low PDIs. Work is currently ongoing to fully understand the steric effects on the nature of the polymerisation.

Experimental Section

General Procedures: For the preparation and characterisation of metal complexes, all reactions and manipulations were performed under an inert atmosphere of argon using standard Schlenk or glovebox techniques. Zr(O*i*Pr)$_4$*i*PrOH (99.9%, Aldrich) and Hf(O*i*Pr)$_4$*i*PrOH (99.9%, Strem) were used without further purification. *rac*-LA (Aldrich) was recrystallised from toluene and sublimed twice prior to use. All other chemicals were purchased from Aldrich. All solvents used in the preparation of metal complexes and polymerisation reactions were dry and obtained from a solvent purification system. ^{1}H and ^{13}C{^{1}H} NMR spectra were recorded with a Bruker 250, 300, 400 or 500 MHz instrument and referenced to residual solvent peaks. Coupling constants are given in Hertz. Elemental analyses were performed by Mr. A. K. Carver at the Department of Chemistry, University of Bath. The ligands were prepared according to standard literature procedures and the purity confirmed by ^{1}H/^{13}C{^{1}H} NMR and HRMS prior to use.[10]

X-ray Crystallography: Crystallographic data are summarised in Table 5. All data were collected with a Nonius Kappa CCD area detector diffractometer [except those for Hf(**4**)(O*i*Pr)$_2$, which were collected with a Xcalibur, Atlas diffractometer] using Mo-K_α radiation (λ = 0.71073 Å) at a temperature of 150(2) K, and all structures were solved by direct methods and refined on all F^2 data using SHELXL-97.[21] Refinement was straightforward with the following noteworthy points: for Zr$_4$(**1**)(O*i*Pr)$_{14}$(HO*i*Pr)$_2$ two isopropoxides [bound to O8 and O9] were disordered in a 50:50 and 65:35 ratio. For Hf$_2$(**1**)(O*i*Pr)$_6$ two isopropoxides [bound to O9 and O10] were left isotropic. In Zr$_2$(**2**)(O*i*Pr)$_6$ the methyl group of the piperazine ring C17 was disordered on two carbon atoms (C15 and C13) in a 50:50 ratio; the hydrogen atoms associated with C15 and C13 are not included in the model, and the carbon atoms of the isopropoxide O6 were more anisotropic than desirable but attempts to model them proved fruitless. In Hf$_2$(**3**)(O*i*Pr)$_6$ the methyl groups of the isopropoxide containing O1 were disordered over two positions in a 75:25 ratio and the methyl groups from one *t*Bu moiety were disordered over two positions in a 60:40 ratio and these were left isotropic. The asymmetric unit for Hf(**4**)(O*i*Pr)$_2$ consisted of two half molecules of hexane. Hydrogen atoms were placed in calculated positions and refined using a riding model, except for **3**H$_2$ and Zr$_4$(**1**)(O*i*Pr)$_{14}$(HO*i*Pr)$_2$ where the OH hydrogen atoms were freely refined. CCDC-829388 [for Zr$_4$(**1**)(O*i*Pr)$_{14}$(HO*i*Pr)$_2$], -829389 [for Hf$_2$(**1**)(O*i*Pr)$_6$], -829390 [for Zr$_2$(**2**)(O*i*Pr)$_6$], -829391 [for Hf$_2$(**3**)-(O*i*Pr)$_6$], -829392 [for Hf(**4**)(O*i*Pr)$_2$], -829398 [for Zr(**5**)(O*i*Pr)$_2$-1/2(C_4H_8O)1/2(C_3H_8O)], -829394 [for Zr(**5**)(O*i*Pr)$_2$], -829393 [for Hf(**5**)(O*i*Pr)$_2$], -829395 [for Zr(**6**)(O*i*Pr)$_2$], -829396 [for Hf(**6**)-(O*i*Pr)$_2$] and -829397 (for **3**H$_2$) contain the supplementary crystallographic data for this paper. These data can be obtained free of charge from The Cambridge Crystallographic Data Centre via www.ccdc.cam.ac.uk/data_request/cif.

Table 5. Crystallographic details for Zr_4(**1**)(O*i*Pr)$_{14}$(HO*i*Pr)$_2$, Hf_2(**1**)(O*i*Pr)$_6$, Zr_2(**2**)(O*i*Pr)$_6$, Hf_2(**3**)(O*i*Pr)$_6$, Hf(**4**)(O*i*Pr)$_2$, Zr(**5**)(O*i*Pr)$_2$, Hf(**5**)(O*i*Pr)$_2$, Zr(**6**)(O*i*Pr)$_2$, Hf(**6**)(O*i*Pr)$_2$ and **3**H_2.

Compound reference	Zr_4(**1**)(O*i*Pr)$_{14}$(HO*i*Pr)$_2$	Hf_2(**1**)(O*i*Pr)$_6$	Zr_2(**2**)(O*i*Pr)$_6$	Hf_2(**3**)(O*i*Pr)$_6$	Hf(**4**)(O*i*Pr)$_2$
Chemical formula	$C_{76}H_{156}N_2O_{18}Zr_4$	$C_{80}H_{140}Hf_4N_4O_{16}$	$C_{47}H_{84}N_2O_8Zr_2$	$C_{26}H_{47}HfNO_4$	$C_{23.50}H_{41}Hf_{0.50}NO_2$
Formula mass	1750.91	2127.92	987.60	616.14	458.82
Crystal system	monoclinic	triclinic	orthorhombic	monoclinic	triclinic
a (Å)	21.8419(4)	12.8800(6)	14.3530(6)	10.3720(5)	8.7915(3)
b (Å)	15.0338(3)	17.1940(9)	39.3260(15)	17.1010(9)	16.8368(6)
c (Å)	29.6284(5)	21.3410(10)	19.3250(7)	16.7140(7)	17.6504(6)
α (°)	90	108.912(2)	90	90	66.874(3)
β (°)	104.829(1)	93.491(3)	90	105.698(3)	79.532(3)
γ (°)	90	93.019(3)	90	90	84.196(3)
Unit cell volume (Å^3)	9404.9(3)	4449.6(4)	10907.9(7)	2854.0(2)	2361.41(14)
Space group	*C*2/*c*	$P\bar{1}$	*C*2*cb*	*Pn*	$P\bar{1}$
Z	4	2	8	4	4
Reflections measured	42398	34810	64279	28088	23772
Independent reflections (R_{int})	7991 (0.0794)	13794 (0.1529)	9549 (0.0949)	10193 (0.0707)	10822 (0.0696)
GoF	1.046	1.023	1.098	1.047	0.979
R_1, wR_2 [$I>2\sigma(I)$]	0.0541, 0.1022	0.0655, 0.1120	0.0536, 0.1273	0.0414, 0.0812	0.0492, 0.0746
R_1, wR_2 [all data]	0.0916, 0.1170	0.1482, 0.1420	0.0889, 0.1513	0.0752, 0.0957	0.0792, 0.0831
Max [min] difference (e Å^{-3})	0.508, –0.653	1.145, –1.315	0.665, –0.561	1.258, –0.748	1.101, –1.352
Compound reference	Zr(**5**)(O*i*Pr)$_2$	Hf(**5**)(O*i*Pr)$_2$	Zr(**6**)(O*i*Pr)$_2$	Hf(**6**)(O*i*Pr)$_2$	**3**H_2
Chemical formula	$C_{29}H_{44}N_2O_4Zr$	$C_{29}H_{44}HfN_2O_4$	$C_{35}H_{56}N_2O_4Zr$	$C_{17.50}H_{26}Hf_{0.50}NO_2$	$C_{35}H_{56}N_2O_2$
Formula mass	575.88	663.15	660.04	371.64	536.82
Crystal system	monoclinic	monoclinic	monoclinic	monoclinic	triclinic
a (Å)	8.5750(6)	8.5680(3)	11.7950(5)	11.7460(2)	10.0750(2)
b (Å)	16.5030(14)	16.4690(7)	24.3760(10)	24.2790(5)	13.3950(3)
c (Å)	20.7000(15)	20.6830(7)	7.6360(4)	7.6000(2)	14.3470(3)
α (°)	90	90	90	90	65.770(1)
β (°)	99.220(5)	99.410(3)	124.476(2)	124.504(1)	88.236(1)
γ (°)	90	90	90	90	71.981(1)
Unit cell volume (Å^3)	2891.5(4)	2879.23(19)	1809.86(14)	1786.10(7)	1668.67(6)
Space group	$P2_1/n$	$P2_1/n$	*Cm*	*Cm*	$P\bar{1}$
Z	4	4	2	4	2
Reflections measured	45579	50883	7278	17045	31837
Independent reflections (R_{int})	6603 (0.0584)	6592 (0.0760)	3018 (0.0452)	4042 (0.0338)	7600 (0.0632)
GoF	1.107	1.185	1.029	1.065	1.034
R_1, wR_2 [$I>2\sigma(I)$]	0.0349, 0.0789	0.0414, 0.0888	0.0360, 0.0799	0.0201, 0.0491	0.0540, 0.1341
R_1, wR_2 [all data]	0.0524, 0.0897	0.0614, 0.0977	0.0394, 0.0816	0.0201, 0.0491	0.0788, 0.1518
Max, min difference (e Å^{-3})	0.417, –0.700	1.963, 1.601	0.462, –0.579	0.789, –1.438	0.320, –0.334

Synthesis of the Ligands: A typical ligand synthesis is as follows for **4**H_2: 2,4-di-*tert*-butylphenol (4.12 g, 20.0 mmol), homopiperazine (1 g, 10.0 mmol) and formaldehyde (38% in H_2O) (1.66 mL, 0.63 g, 21.0 mmol) were heated to reflux in MeOH (40 mL) for 24 h then cooled (0 °C). During which time a white precipitate was observed, which was collected by filtration, washed with cold MeOH and dried to yield a white solid (1.29 g, 2.4 mmol, 24%). ^{1}H NMR ($CDCl_3$): δ = 1.32 (s, 18 H, *t*Bu), 1.47 (s, 18 H, *t*Bu), 1.95 (quin, J = 6.1 Hz, 2 H, ring-CH_2), 2.81 (s, 4 H, ring-CH_2), 2.78 (t, J = 6.0 Hz, 4 H, ring-CH_2), 3.81 (s, 4 H, NCH_2Ar), 6.86 (d, J = 2.3 Hz, 2 H, ArH), 7.26 (d, J = 2.3 Hz, 2 H, ArH), 11.03 (br, 2 H, OH) ppm. $^{13}C\{^1H\}$ NMR ($CDCl_3$): δ = 26.9 (CH_2), 29.8 (CH_3), 31.8 (CH_3), 34.3 (C), 35.0 (C), 53.2 (CH_2), 54.6 (CH_2), 62.6 (CH_2), 121.4 (Ar), 123.1 (ArH), 123.6 (ArH), 135.8 (Ar), 140.7 (Ar), 154.4 (ArO) ppm. Calc. *m*/*z* $[C_{35}H_{56}N_2O_2 + H]^+$ 537.4420; found 537.4442.

Synthesis and Characterisation of the Complexes: A typical example for the preparation of a complex is as follows for Hf(**4**)(O$_i$Pr)$_2$: **4**H_2 (0.53 g, 0.99 mmol) and Hf(O*i*Pr)$_4$·*i*PrOH (0.47 g, 0.99 mmol) were dissolved in CH_2Cl_2 (30 mL) and stirred for 16 h. The solvent was removed in vacuo, and the residue was recrystallised from hot hexane (40 mL) to yield colourless crystals (0.14 g, 0.17 mmol, 17%). ^{1}H NMR ($CDCl_3$, 233 K): δ = –0.02 (d, J = 6.0 Hz, 6 H, Me), 1.18 (d, J = 6.0 Hz, 6 H, *t*Bu), 1.20 (s, 18 H, *t*Bu), 1.40 (s, 18 H, *t*Bu), 1.79 (br, 1 H, CH_2), 2.19 (br, 1 H, CH_2), 2.44 (br, 2 H, CH_2), 2.95 (d, J = 6.5 Hz, 2 H, CH_2), 3.17 (d, J = 11.5 Hz, 2 H, CH_2), 3.52 (d, J = 6.5 Hz, 2 H, CH_2), 3.63 (br, 2 H, NCH_2Ar), 3.63 (br, 1 H, CH), 4.32 (d, J = 11.5 Hz, 2 H, NCH_2Ar), 4.32 (br, 1 H, CH), 6.86 (s, 2 H, ArH), 7.24 (s, 2 H, ArH) ppm. $^{13}C\{^1H\}$ NMR ($CDCl_3$, 258 K): δ = 22.6 (CH_2), 25.8 (CH_3), 27.5 (CH_3), 30.0 (CH_3), 31.8 (CH_3), 34.0 (C), 35.1 (C), 54.5 (CH_2), 56.3 (CH_2), 63.7 (CH_2), 68.0 (CH), 69.0 (CH), 122.6 (Ar), 124.5 (ArH), 124.6 (ArH), 136.3 (Ar), 136.3 (Ar), 137.6 (Ar), 161.3 (ArO) ppm. $C_{41}H_{68}HfN_2O_4$ (831.49): calcd. C 59.22, H 8.24, N 3.37; found C 59.8, H 8.26, N 3.68.

Polymerisation Procedure: For solvent-free polymerisations the monomer:initiator ratio employed was 300:1 (unless otherwise stated) at a temperature of 130 °C, in all cases 1 g of *rac*-LA was used. After the reaction time methanol (20 mL) was added to quench the reaction and the resulting solid was dissolved in dichloromethane. The solvents were removed in vacuo and the resulting solid was washed with copious amounts of methanol to remove any unreacted monomer. ^{1}H NMR spectroscopy ($CDCl_3$) and GPC (THF) were used to determine tacticity and molecular weights (M_n and M_w) of the polymers produced; P_m (the probability of isotactic linkages) was determined by analysis of the methine region of the homonuclear decoupled ^{1}H NMR spectra. The equations used to calculate P_r and P_m are given by Coates et al.[1a] Gel permeation

chromatography (GPC) analyses were performed on a Polymer Laboratories PL-GPC 50 integrated system using a PLgel 5 μm MIXED-D 300 × 7.5 mm column at 35 °C, THF solvent (flow rate, 1.0 mL/min). The polydispersity index (PDI) was determined from M_w/M_n, where M_n is the number average molecular weight and M_w the weight average molecular weight. The polymers were referenced to 11 narrow molecular weight polystyrene standards with a range of M_w 615–568,000 Da.

Supporting Information (see footnote on the first page of this article): GPC chromatograms, full experimental procedures and further kinetic details.

Acknowledgments

We gratefully acknowledge the Engineering and Physical Sciences Research Council (EPSRC) for the National Mass Spectrometry Service Centre Swansea and the University of Bath for funding.

[1] a) B. M. Chamberlain, M. Cheng, D. R. Moore, T. M. Ovitt, E. B. Lobkovsky, G. W. Coates, *J. Am. Chem. Soc.* **2001**, *123*, 3229–3238; b) M. H. Chisholm, N. W. Eilerts, J. C. Huffman, S. S. Iyer, M. Pacold, K. Phomphrai, *J. Am. Chem. Soc.* **2000**, *122*, 11845–11854; c) A. J. Chmura, M. G. Davidson, M. D. Jones, M. D. Lunn, M. F. Mahon, A. F. Johnson, P. Khunkamchoo, S. L. Roberts, S. S. F. Wong, *Macromolecules* **2006**, *39*, 7250–7257; d) O. Dechy-Cabaret, B. Martin-Vaca, D. Bourissou, *Chem. Rev.* **2004**, *104*, 6147–6176; e) Y. Kim, G. K. Jnaneshwara, J. G. Verkade, *Inorg. Chem.* **2003**, *42*, 1437–1447; f) B. J. O'Keefe, M. A. Hillmyer, W. B. Tolman, *J. Chem. Soc., Dalton Trans.* **2001**, 2215–2224; g) T. M. Ovitt, G. W. Coates, *J. Am. Chem. Soc.* **2002**, *124*, 1316–1326; h) M. D. Jones, M. G. Davidson, C. G. Keir, L. M. Hughes, M. F. Mahon, D. C. Apperley, *Eur. J. Inorg. Chem.* **2009**, 635–642.

[2] E. T. H. Vink, K. R. Rabago, D. A. Glassner, P. R. Gruber, *Polym. Degrad. Stab.* **2003**, *80*, 403–419.

[3] a) A. C. Albertsson, I. K. Varma, *Biomacromolecules* **2003**, *4*, 1466–1486; b) R. E. Drumright, P. R. Gruber, D. E. Henton, *Adv. Mater.* **2000**, *12*, 1841–1846.

[4] a) A. P. Dove, *Chem. Commun.* **2008**, 6446–6470; b) M. J. Stanford, A. P. Dove, *Chem. Soc. Rev.* **2010**, *39*, 486–494.

[5] a) Y. Huang, Y. H. Tsai, W. C. Hung, C. S. Lin, W. Wang, J. H. Huang, S. Dutta, C. C. Lin, *Inorg. Chem.* **2010**, *49*, 9416–9425; b) L. Wang, X. B. Pan, L. H. Yao, N. Tang, J. C. Wu, *Eur. J. Inorg. Chem.* **2011**, 632–636; c) A. Garces, L. F. Sanchez-Barba, C. Alonso-Moreno, M. Fajardo, J. Fernandez-Baeza, A. Otero, A. Lara-Sanchez, I. Lopez-Solera, A. M. Rodriguez, *Inorg. Chem.* **2010**, *49*, 2859–2871; d) X. Xu, Y. F. Chen, G. Zou, Z. Ma, G. Y. Li, *J. Organomet. Chem.* **2010**, *695*, 1155–1162; e) J. C. Wu, Y. Z. Chen, W. C. Hung, C. C. Lin, *Organometallics* **2008**, *27*, 4970–4978; f) M. G. Cushion, P. Mountford, *Chem. Commun.* **2011**, *47*, 2276–2278; g) E. Grunova, E. Kirillov, T. Roisnel, J. F. Carpentier, *Dalton Trans.* **2010**, *39*, 6739–6752; h) H. Y. Ma, T. P. Spaniol, J. Okuda, *Angew. Chem. Int. Ed.* **2006**, *45*, 7818–7821.

[6] a) H. Ma, T. P. Spaniol, J. Okuda, *Inorg. Chem.* **2008**, *47*, 3328–3339; b) Y. J. Luo, X. L. Wang, J. Chen, C. C. Luo, Y. Zhang, Y. M. Yao, *J. Organomet. Chem.* **2009**, *694*, 1289–1296; c) J. F. Wang, Y. M. Yao, Y. Zhang, Q. Shen, *Inorg. Chem.* **2009**, *48*, 744–751; d) Z. J. Zhang, X. P. Xu, W. Y. Li, Y. M. Yao, Y. Zhang, Q. Shen, Y. J. Luo, *Inorg. Chem.* **2009**, *48*, 5715–5724; e) P. L. Arnold, J. C. Buffet, R. P. Blaudeck, S. Sujecki, A. J. Blake, C. Wilson, *Angew. Chem. Int. Ed.* **2008**, *47*, 6033–6036.

[7] a) L. M. Alcazar-Roman, B. J. O'Keefe, M. A. Hillmyer, W. B. Tolman, *Dalton Trans.* **2003**, 3082–3087; b) M. H. Chisholm, N. J. Patmore, Z. P. Zhou, *Chem. Commun.* **2005**, 127–129; c) N. Nomura, A. Akita, R. Ishii, M. Mizuno, *J. Am. Chem. Soc.* **2010**, *132*, 1750–1751; d) N. Nomura, R. Ishii, Y. Yamamoto, T. Kondo, *Chem. Eur. J.* **2007**, *13*, 4433–4451; e) Z. Y. Zhong, P. J. Dijkstra, J. Feijen, *Angew. Chem. Int. Ed.* **2002**, *41*, 4510–4513; f) Z. Y. Zhong, P. J. Dijkstra, J. Feijen, *J. Am. Chem. Soc.* **2003**, *125*, 11291–11298.

[8] a) I. Peckermann, A. Kapelski, T. P. Spaniol, J. Okuda, *Inorg. Chem.* **2009**, *48*, 5526–5534; b) A. Pietrangelo, M. A. Hillmyer, W. B. Tolman, *Chem. Commun.* **2009**, 2736–2737; c) J. C. Buffet, J. Okuda, P. L. Arnold, *Inorg. Chem.* **2010**, *49*, 419–426; d) A. Pietrangelo, S. C. Knight, A. K. Gupta, L. J. Yao, M. A. Hillmyer, W. B. Tolman, *J. Am. Chem. Soc.* **2010**, *132*, 11649–11657; e) M. P. Blake, A. D. Schwarz, P. Mountford, *Organometallics* **2011**, *30*, 1202–1214.

[9] a) T. K. Saha, V. Ramkumar, D. Chakraborty, *Inorg. Chem.* **2011**, *50*, 2720–2722; b) A. D. Schwarz, K. R. Herbert, C. Paniagua, P. Mountford, *Organometallics* **2010**, *29*, 4171–4188; c) E. L. Whitelaw, M. D. Jones, M. F. Mahon, *Inorg. Chem.* **2010**, *49*, 7176–7181; d) M. G. Hu, M. Wang, H. J. Zhu, L. Zhang, H. Zhang, L. C. Sun, *Dalton Trans.* **2010**, *39*, 4440–4446; e) M. D. Jones, M. G. Davidson, G. Kociok-Kohn, *Polyhedron* **2010**, *29*, 697–700; f) C. Romain, L. Brelot, S. Bellemin-Laponnaz, S. Dagorne, *Organometallics* **2010**, *29*, 1191–1198; g) T. K. Saha, B. Rajashekhar, R. R. Gowda, V. Ramkumar, D. Chakraborty, *Dalton Trans.* **2010**, *39*, 5091–5093; h) E. Sergeeva, J. Kopilov, I. Goldberg, M. Kol, *Inorg. Chem.* **2010**, *49*, 3977–3979.

[10] S. L. Hancock, M. F. Mahon, M. D. Jones, *Dalton Trans.* **2011**, *40*, 2033–2037.

[11] A. L. Zelikoff, J. Kopilov, I. Goldberg, G. W. Coates, M. Kol, *Chem. Commun.* **2009**, 6804–6806.

[12] C. K. A. Gregson, I. J. Blackmore, V. C. Gibson, N. J. Long, E. L. Marshall, A. J. P. White, *Dalton Trans.* **2006**, 3134–3140.

[13] a) S. Gendler, A. L. Zelikoff, J. Kopilov, I. Goldberg, M. Kol, *J. Am. Chem. Soc.* **2008**, *130*, 2144–2145; b) E. Sergeeva, J. Kopilov, I. Goldberg, M. Kol, *Chem. Commun.* **2009**, 3053–3055; c) A. Yeori, I. Goldberg, M. Shuster, M. Kol, *J. Am. Chem. Soc.* **2006**, *128*, 13062–13063; d) S. Gendler, S. Segal, I. Goldberg, Z. Goldschmidt, M. Kol, *Inorg. Chem.* **2006**, *45*, 4783–4790.

[14] F. H. Allen, *Acta Crystallogr., Sect. B-Struct. Sci.* **2002**, *58*, 380–388.

[15] a) G. Ciancaleoni, N. Fraldi, P. H. M. Budzelaar, V. Busico, A. Macchioni, *Organometallics* **2011**, *30*, 100–114; b) G. Ciancaleoni, N. Fraldi, P. H. M. Budzelaar, V. Busico, A. Macchioni, *Dalton Trans.* **2009**, 8824–8827.

[16] a) R. Mayilmurugan, M. Sankaralingam, E. Suresh, M. Palaniandavar, *Dalton Trans.* **2010**, *39*, 9611–9625; b) M. Du, X. J. Zhao, J. H. Guo, X. H. Bu, J. Ribas, *Eur. J. Inorg. Chem.* **2005**, 294–304.

[17] R. Cariou, V. C. Gibson, A. K. Tomov, A. J. P. White, *J. Organomet. Chem.* **2009**, *694*, 703–716.

[18] E. L. Whitelaw, M. D. Jones, M. F. Mahon, G. Kociok-Kohn, *Dalton Trans.* **2009**, 9020–9025.

[19] I. R. Thomas, I. J. Bruno, J. C. Cole, C. F. Macrae, E. Pidcock, P. A. Wood, *J. Appl. Crystallogr.* **2010**, *43*, 362–366.

[20] a) M. Wang, H. J. Zhu, D. G. Huang, K. Jin, C. N. Chen, L. C. Sun, *J. Organomet. Chem.* **2004**, *689*, 1212–1217; b) F. Corazza, E. Solari, C. Floriani, A. Chiesivilla, C. Guastini, *J. Chem. Soc., Dalton Trans.* **1990**, 1335–1344.

[21] G. M. Sheldrick, *Acta Crystallogr., Sect. A* **2008**, *64*, 112–122.

Received: June 13, 2011
Published Online: September 5, 2011

